Iranian Journal of Physics Research, Vol. 21, No. 3, 2021

Monte Carlo Simulation and Experimental Determination of Tissue Phantom Ratio for Photon Beams delivered from Medical Linear Accelerator

N M Rasel[1], S. Purohit[2], M S Rahman[3], AKM M H Meaze[2*] and M Y Ali[4]
1. Department of Physics, Comilla University, Cumilla- 3506, Bangladesh
2. Department of Physics, University of Chittagong, Chattogram- 4331, Bangladesh
3. Secondary Standard Dosimetry Laboratory, Institute of Nuclear Science & Technology, Bangladesh Atomic Energy Commission, Savar, Dhaka- 1100, Bangladesh
4. Department of Physics, University of Rajshahi, Rajshahi, Bangladesh

E-mail: meaze@cu.ac.bd

(Received 25 March 2021 ; in final form 24 May 2021)

Abstract
For an external radiotherapy procedure, the tissue phantom ratio ($TPR_{20,10}$) is used as a photon beam quality index. This work presents an estimate of $TPR_{20,10}$ using two cylindrical ionization chambers (NE2571 Farmer and PTW30013) in three high-energy photon modes (6, 10 and 15 MV) using both the Monte Carlo simulation and the experimental setup. The MCNPX (version 2.6.0) was used for the simulation of photon beams delivered by Varian-2300CD linac for the determination of $TPR_{20,10}$ according to technical report series (TRS) 398. Again, applying the same protocol $TPR_{20,10}$ values were measured experimentally with NE2571 Farmer and PTW30013 chambers for the same medical linear accelerator (LINAC). The differences of $TPR_{20,10}$ between MCNPX and experimental values were found for NE2571 Farmer chamber within 4.17 percent, 2.9 percent and 2.5 percent and similarly, these were within 3.89 percent, 2.71 percent and 1.98 percent at 6, 10 and 15 MV respectively for PTW30013. The $TPR_{20,10}$ values simulated by MCNPX demonstrated close agreement with our experimental results.

Keywords: Tissue Phantom Ratio (TPR), TRS-398, Monte Carlo simulation

1. Introduction
Radiotherapy is one of the most efficient and reliable treatment modalities for the management of cancer patient. Today more than 50% patient are treated with radiation therapy [1-2]. Modern RT technique often uses high energy photon beam from medical linear accelerators for the irradiation of deeply located cancer cells. It is because the high energy photon beam provides lower surface dose where depth doses are higher and a lower scatter dose outside of the treatment field which are essential for the management of deep cancer tumor [3].

The photon beam spectra produced by a clinical linear accelerator is very essential for numerous dosimetric studies. However, it is not easier to measure the spectra for megavoltage photon beam. Moreover, various dosimetric quantities like wall correction factor, stopping power ratio, central electrode correction factor, etc. depend upon the quality of the incident photon beam [4]. In the medical radiotherapy photon energy range, the main photon beam quality indices are $TPR_{20,10}$, percentage depth dose $PDD(10)_x$ and d_{80},etc. However, most of the dosimetry protocols (IPEM, IAEA TRS-398, etc) based on absorbed dose to water calibration using $TPR_{20,10}$, as photon beam quality index [5-8]. The parameter $TPR_{20,10}$ is defined as the ratio of absorbed doses on the beam axis at depth of 20 cm and 10 cm in a water phantom, obtained with a constant source-chamber distance (SCD) of 100 cm and 10 cm × 10 cm field size at the detector position of the water phantom. The most important characteristic of the beam quality parameter $TPR_{20,10}$ is its independence of the electron contamination in the incident beam [9-12].

There are some studies on TPR by using several Monte Carlo codes. A paper by Fonseca et al. [13] presented TPR for 6 MV photon beam by MCNP 6, EGSnrc, and PENELOPE MC codes. In that work, authors used a simplified MC model which contains a point photon source spectrum (extracted from the previously published works), X & Y-jaws, and a water

Figure 1. 2-D simulation geometry of linac including water phantom.

phantom. They also performed experimental measurements by using PTW30013 chamber. Monte Carlo and experimental values were 0.67 and 0.667 respectively. In another work by Wulff et al. [14] determined beam quality specifier for several photon beams using egs chamber user code. They also used published megavoltage photon beam spectra as source particles. They computed TPR for 4 MV, 6MV, 18MV, and 24 MV as 0.621, 0.662, 0.780, 0.806 respectively and uncertainty were within 0.3%. Baumgartner et al. [15] calculated the photon energy spectra as well as TPR for Varian 2100C and 2300C/D by using PENELOPE MC code. In their work, TPR values were computed as 0.601, 0.665, and 0.735 for 4MV,6MV, and 10 MV respectively and uncertainty were within 2.6%. Moreover, they considered a simplified model of source electron. After close investigation of previously published literatures, we found that there is lack of study of the detailed simulation of medical linac for direct determination of tissue phantom ratio. Moreover, most of the works used EGSnrc and PENELOPE MC codes to obtain TPR values.

In this work, we present the tissue phantom ratio (TPR) for 6 MV, 10 MV, and 15 MV photon beam from Varian clinac using MCNP Monte Carlo code by detailed simulation of the geometry of linac and validates the MC obtained results with experimental measurements carried out by two thimble type cylindrical ion chambers.

1. Materials and Methods

2.1 Monte Carlo simulation

To perform a simulation in MCNP, it is needed to write the input files describing the geometry, the materials used, the particles of interest, the physical process of interaction and the function main that indicates where the program will start and manage its execution [16-21]. The MC simulation of the accelerator head of a medical LINAC was performed by MCNPX MC code. The following sections describe the geometry of several components used in this simulation.

2.1.1 Accelerator geometry

In this research work, the head structure of Varian Clinac (model 2300 C/D) was simulated by using MCNPX (version 2.6.0) Monte Carlo code [22]. The major components of linac head such as, Bremsstrahlung target (converter), absorber (electron stopper), primary conical collimator, flattening filter, and the treatment field defining secondary collimators (jaws) were modeled in this study. The materials compositions (density) and dimensions of these components were collected from the technical drawing of linac provided by Varian medical system. The target of the medical LINAC was defined as two cylinders, one made of tungsten and the other was copper. The primary collimator is made of tungsten, about 7.47 cm thickness, located just below the x-ray target. The conical- shaped flattening filter provided uniform radiation intensity distribution across X-ray fields at any depth of treatment. There was also a unique specification of the FF dimension for each photon beam. The secondary collimators consisted of two pairs of jaws, one above the other. The pair of jaws was made of tungsten of about 7.77 and 7.80 cm thickness respectively.

Figure 1 shows the simulated head diagram of Varian 2300 C/D Clinac. Moreover, the source electron (primary electron beam) which impinges perpendicularly on the target (converter) to produce Bremsstrahlung photons was defined as monodirectional and monoenergetic beam with 5 mm beam radius. Besides, a standard IAEA cubic water phantom (30 cm × 30 cm × 30 cm) was also simulated at 100 cm distance from the target location to obtain the dose distribution within phantom.

2.1.2 Ion chamber geometry

Two thimble type cylindrical ionization chambers were modeled by declaring necessary materials and dimensions in the input file of MCNPX code. The dimensions of the chambers were taken from the IAEA TRS-398 protocol [23]. The NE2571 chamber cavity had a diameter of 0.64 cm and a length of 2.4 cm and includes a central electrode with 0.1 cm diameter. The wall of this chamber was made of graphite with 0.065 g.cm^{-2} thickness. As this chamber was non-waterproof, a waterproofing sleeve made of 1.0 mm PMMA was also used. The air gap of 0.1 mm between the chamber wall and waterproofing sleeve was taken to allow the air pressure in the chamber to equilibrate. Although the necessary dimensions of the NE2571 Farmer chamber were given in the IAEA TRS-398 protocol, the chamber stem material might be different for different Farmer-like chambers. In this case, we modeled the chamber stem material using PMMA as also used by Ma and Nahum [24].

The 0.6 cm^3 PTW30013 chamber was also modeled by taking necessary materials and dimensions from IAEA TRS-398 protocols [23]. The chamber cavity had a diameter of 0.62 cm and a length of 2.3 cm and includes a 2.05 cm central electrode of aluminum with 0.1 cm diameter. The wall material was of PMMA with 0.057 g.cm^{-2} thickness. The remaining parts were used as the same as the NE2571 chamber. The sensitive volume of each chamber was filled with ambient air of 0.001225 g.cm^{-3} density.

Besides ion chambers, IAEA standard cubic water phantom with dimensions 30 × 30 × 30 cm^3 was also

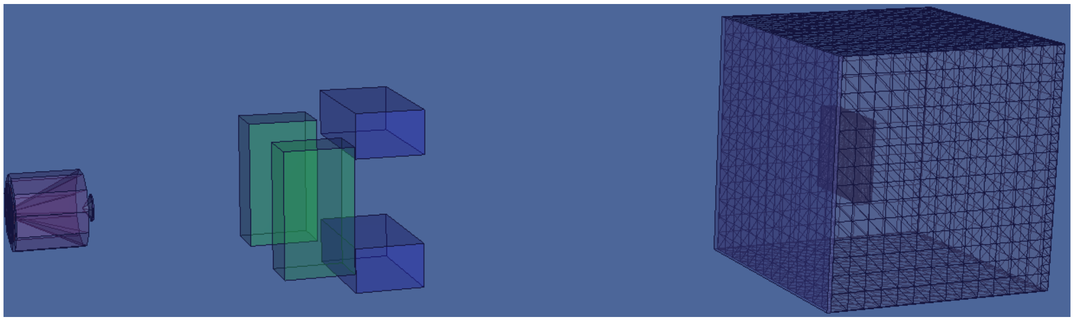

Figure 2. 3-D geometry of linac for photon dose calculations.

Figure 3. Experimental set-up for measuring $TPR_{20,10}$.

modeled. The complete geometry for photon dose calculations is illustrated in Figure 2.

2.1.3 Simulation strategy: calculation of $TPR_{20,10}$

The F4 tally was used to calculate the dose rate (Gy/hr) in chamber sensitive volume. As the F4 tally scores average flux in a cell, the ICRP 21 photon flux to dose conversion factors [25] was employed to obtain dose values by using dose energy (DE) and dose function DF(E) (rem/hr)/(p/cm^2-s) cards. Moreover, the tally multiplier FM4 card was used to incorporate the beam current (particle rate) which was 1E10. Since the quality factor for X-ray photon is one so the resultant tally is equivalent to the unit of absorbed dose. The modified F4 tally score the dose value per source particle. A number of input files were run with NPS at least 3E8 till the R-value (relative error) were within 0.1 and passes 10 statistical tests. Dose values were computed at 20 cm and 10 cm depth of water phantom with SCD 100 cm and field size 100 cm^2 at chamber location. In addition, the tally energy card E4 was also used to see the dose score by individual energy bin. To reduce the computing time, IMP card was employed as variance reduction technique.

2.2 Experimental Measurement of $TPR_{20,10}$

Experimental tissue phantom ratio ($TPR_{20,10}$) was determined for 6 MV, 10 MV, and 15 MV photon beam from Varian linac (2300C/D) at the National Institute of Cancer Research & Hospital (NICRH) in Dhaka, Bangladesh. Measurements were performed using IAEA standard cubic water phantom and two cylindrical ion chambers NE2571 and PTW30013 with 0.6 cc sensitive volume. These ion chambers were connected to a IBA dose-1 dosimeter. The calibration of these chambers was done in Secondary Standard Dosimetry Laboratory (SSDL), Bangladesh. The water phantom was placed below the linac gantry and the ion chamber was immersed at 10 cm and 20 cm depth of water phantom respectively. The set-up consists of 100 cm SCD (Source to Chamber Distance) and 100 cm^2 field size at detector location. The reference conditions of experimental measurements were according to TRS-398 protocol [15]. The $TPR_{20,10}$ was calculated using the following equations

$$TPR_{20,10} = \frac{M_{raw,20,Q}}{M_{raw,10,Q}} \quad (1)$$

Where $Mraw_{,20,Q}$ and $Mraw_{,10,Q}$ are the ion chamber reading (nC) at depths of 20 cm and 10 cm, respectively. Figure 3 shows the experimental set-up used for the measurements.

3. Results

3.1 Monte Carlo calculated values of $TPR_{20,10}$

Monte Carlo calculated dose- energy data were plotted (dose rate per unit energy vs energy) for each photon mode and ionization chamber. The total dose rate at 20 cm and 10 cm depth of water phantom at the reference

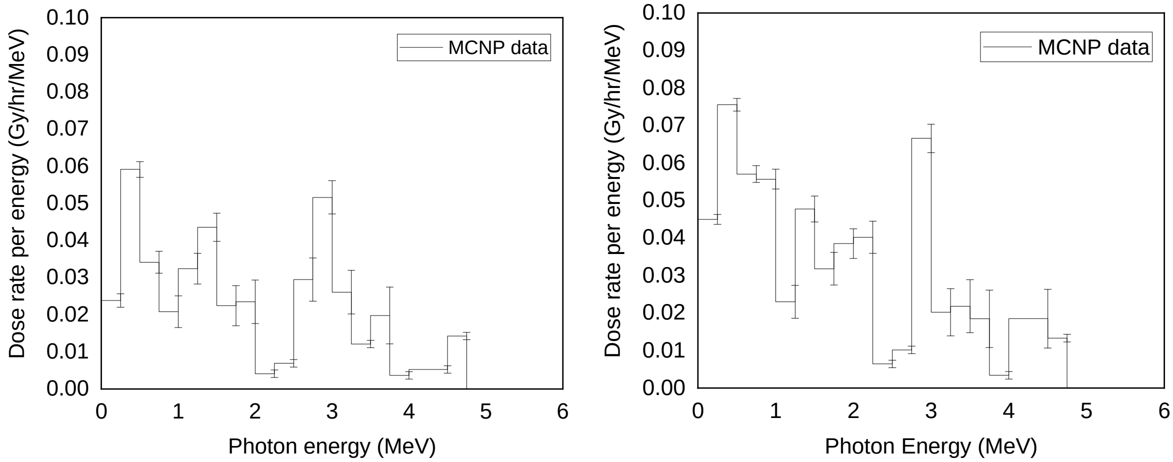

(a) (b)

Figure 4. Dose energy spectrum of 6 MeV photon beam at (a) 20 cm and (b) 10 cm depth of water phantom for NE2571 Farmer Chamber.

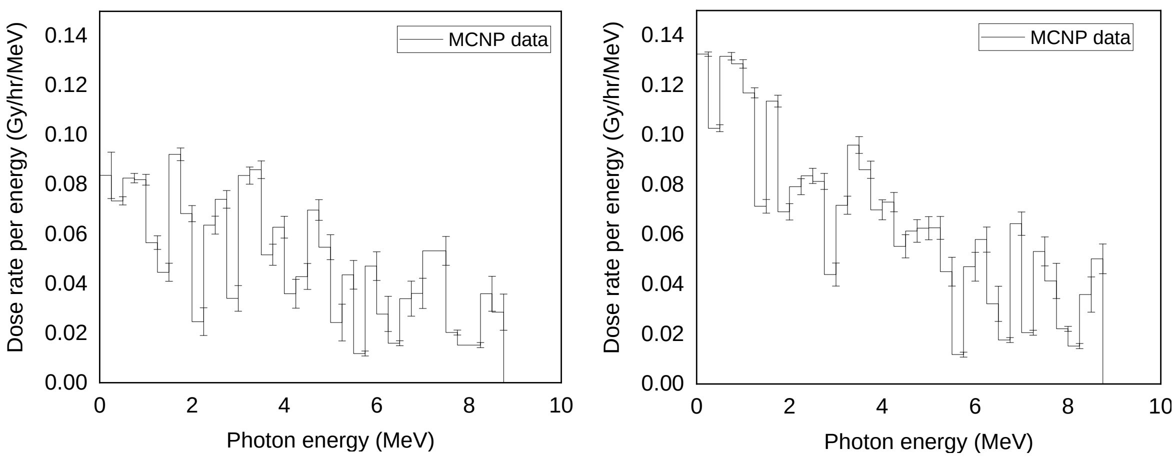

(a) (b)

Figure 5. Dose energy spectrum of 10 MeV photon beam at (a) 20 cm and (b) 10 cm depth of water phantom for NE2571 Farmer Chamber.

point of chamber were taken from the MCNPX output file for each photon beam.

NE2571 Farmer Chamber

Using Figure 4 the dose rate for 6 MV photon beam at two depths of water phantom at SCD 100 cm were calculated and given by

$$\dot{D}_{20} = 0.414664 \pm 0.122500 \left[\text{Gy.hr}^{-1}\right] \text{and}$$

$$\dot{D}_{10} = 0.593459 \pm 0.099100 \left[\text{Gy.hr}^{-1}\right]$$

Taking the ratio of the above two equations, we obtained MC $TPR_{20,10}$ for 6 MV photon beam as .

Using Figure 5 the dose rate for 10 MV photon beam at two depths of water phantom were calculated and given by

$$\dot{D}_{20} = 1.6611000.075800 \left[\text{Gy.hr}^{-1}\right] \text{ and}$$

$$\dot{D}_{10} = 2.308550 \pm 0.064000 \left[\text{Gy.hr}^{-1}\right]$$

The $TPR_{20,10}$ for 10 MV photon beam was obtained by taking the ratio of these two values $TPR_{20,\,10} = 0.7190.018$ From Figure 6 the dose rate for 15 MV photon beam at 20 cm and 10 cm depth of water phantom were obtained as 3.963460 ± 0.057200 [Gy.hr^{-1}] and 5.094420 ± 0.051900 [Gy.hr^{-1}] respectively. Taking the ratio of these value, the $TPR_{20,\,10}$ for 15 MV was found 0.778 ± 0.004.

PTW30013 chamber

The MC calculated dose rate from Figure 7 for 6 MV photon beam at 20 cm and 10 cm depth of water phantom were 0.410123 ± 0.128000 [Gy.hr^{-1}] and 0.590955 ± 0.103700 [Gy.hr^{-1}] respectively. Accordingly, $TPR_{20,10}$ was obtained as 0.694 ± 0.014 for 6 MV photon beam.

The total dose rate of 10 MV photon beam from Figure 8 were calculated and given as 1.662930 ± 0.079000 [Gy.hr^{-1}] and 2.317890 ± 0.066500 [Gyhr^{-1}] for 20 cm and 10 cm depth of water phantom respectively. So, the MC calculated tissue phantom ratio for 10 MV photon was 0.717 ± 0.019.

From Figure 9 the MC calculated dose rate for 15 MV photon mode at 20 and 10 cm depth of water were

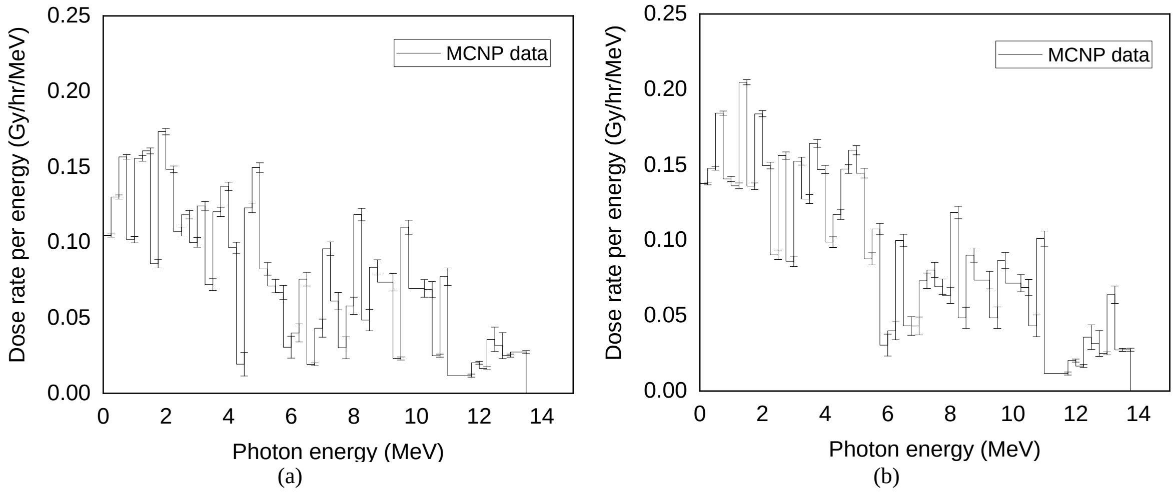

Figure 6. Dose energy spectrum of 15 MeV photon beam at (a) 20 cm and (b) 10 cm depth of water phantom for NE2571 Farmer Chamber.

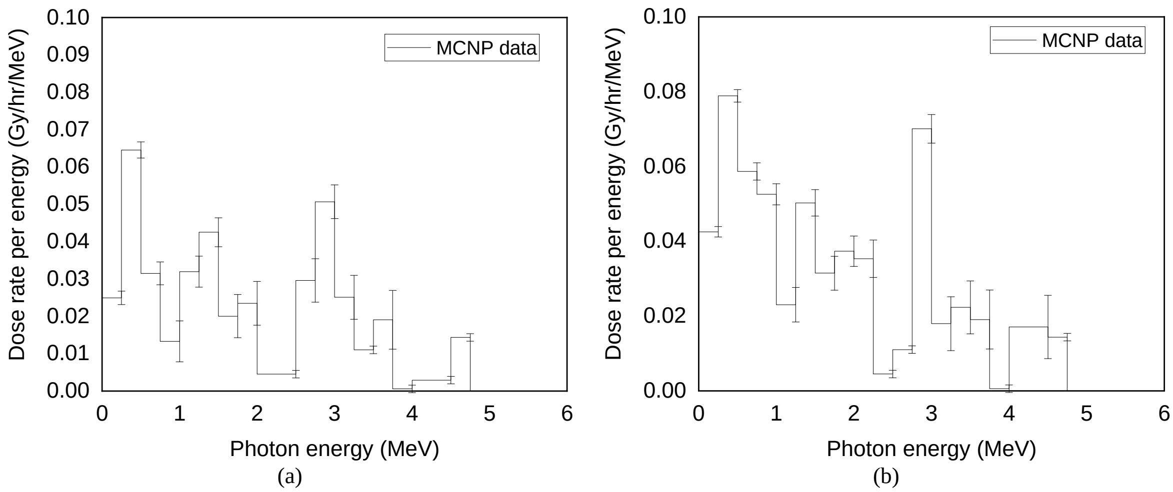

Figure 7. Dose energy spectrum of 6 MeV photon beam at (a) 20 cm and (b) 10 cm depth of water phantom for PTW30013 chamber.

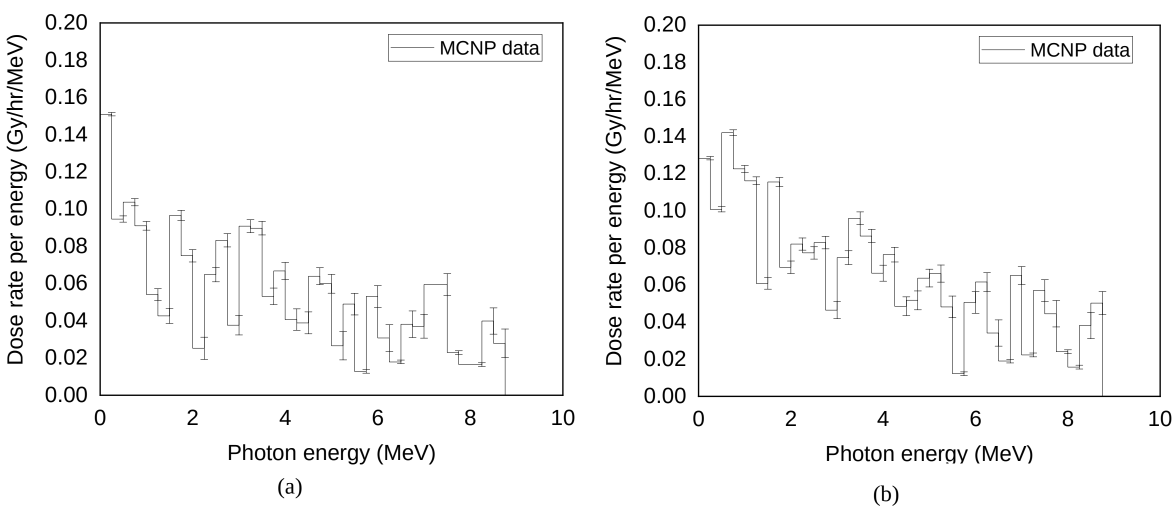

Figure 8. Dose energy spectrum of 10 MeV photon beam at (a) 20 cm and (b) 10 cm depth of water phantom for PTW30013 chamber.

3.922410 ± 0.062400 [$Gy.hr^{-1}$] and 5.074340 ± 0.079800 [$Gy.hr^{-1}$] respectively. Using these data, the tissue phantom ratio was obtained 0.772 ± 0.001.

3.2 Experimental values of $TPR_{20,10}$

Using photon beam from Varian 2300CD medical LINAC following IAEA TRS-398 protocol [01] $TPR_{20,10}$ values

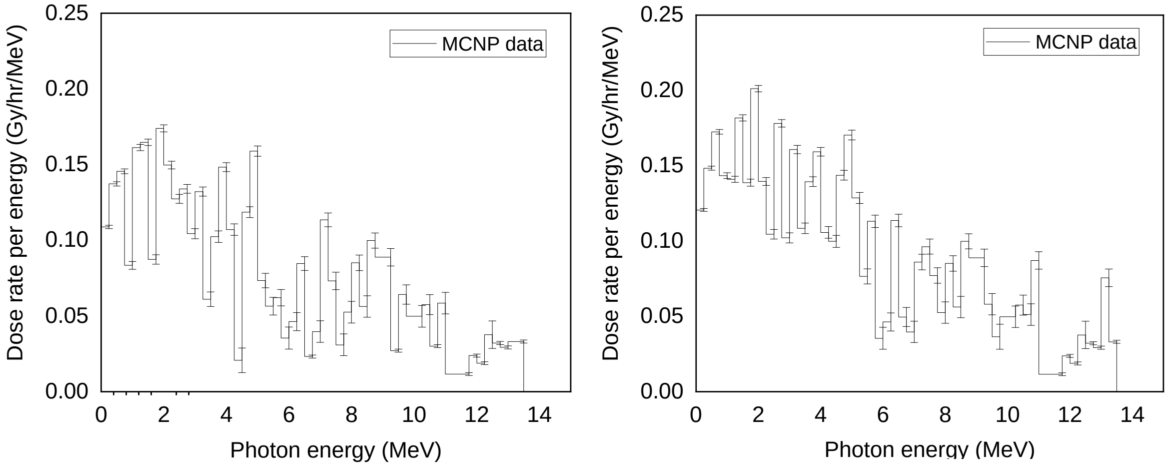

(a) (b)

Figure 9. Dose energy spectrum of 15 MeV photon beam using PTW30013 chamber at (a) 20 cm and (b) 10 cm depth of water phantom.

Table 1. Experimental measurement of $TPR_{20,10}$.

Chamber	Serial number	Tube Voltage (MV)	$M_{raw,20,Q}$ (nC)	$M_{raw,10,Q}$ (nC)	$TPR_{20,10}$
NE2571	1205	6	23.61	35.18	0.671 ± 0.004
		10	29.05	39.21	0.741 ± 0.009
		15	15.45	20.34	0.759 ± 0.004
PTW30013	0364	6	19.93	29.82	0.668 ± 0.005
		10	24.56	33.31	0.737 ± 0.007
		15	13.09	17.30	0.757 ± 0.005

Table 2. Comparison of Experimental and MC calculated values of $TPR_{20,10}$.

Chamber	Tube Voltage (MV)	Experimental $TPR_{20,10}$	MC calculated $TPR_{20,10}$	Difference between simulated and experimental values
NE2571	6	0.671 ± 0.004	0.699 ± 0.013	4 %
	10	0.741 ± 0.009	0.719 ± 0.018	3 %
	15	0.759 ± 0.004	0.778 ± 0.004	2.5 %
PTW30013	6	0.668 ± 0.005	0.694 ± 0.014	3.7 %
	10	0.737 ± 0.007	0.717 ± 0.019	2.7 %
	15	0.757 ± 0.005	0.772 ± 0.001	2%

were measured experimentally and listed in Table 1.
Table 2 shows the comparison between experimental and MC calculated values of $TPR_{20, 10}$.

4. Discussions

The experimentally measured values of $TPR_{20, 10}$ shows dependency on the energy of incident photon beam. The $TPR_{20,10}$ values also vary with the internal structural materials of ionization chambers. It is because the geometric dimensions and materials are not same for all chambers. Particularly, wall material and central electrode have greater impact on the photon interactions and electron interactions produced in the surrounding medium (water). However, the influence of materials on $TPR_{20,10}$ values is very small.

5. Conclusions

For the determination of Tissue Phantom Ratio, $TPR_{20,10}$ for 6, 10 and 15 MV photon modes, we performed both Monte Carlo simulation and experimental measurements using two cylindrical ionization chambers, NE2571 Farmer and PTW30013. Within the parameters of the International Code of Radiological Units (ICRU) recommendation, the simulated and experimental values are in good agreement with each other.

6. List of Abbreviations

Tissue phantom ratio ($TPR_{20,10}$), Monte Carlo N-Particle EXtended (MCNPX), Technical Report Series (TRS), Linear accelerator (LINAC), Percentage Depth Dose $PDD(10)_x$, Source-chamber distance (SCD).

7. Acknowledgement

The corresponding author gratefully acknowledges the project funding support of the Research and Publication Cell, University of Chittagong, Chittagong 4331, Bangladesh.

References

1. R Baskar, K A Lee, R Yeo, and K-W Yeoh, *Cancer and Radiation Therapy: Current Advances and Future Directions*, *Int. J. Med. Sci*. **9** (2012) 3193.
2. A C Begg, F A Stewart, and C Vens, *Strategies to improve radiotherapy with targeted drugs, Nat. Rev. Cancer* **11** (2011) 239.
3. G Delaney, S Jacob, C Featherstone, and M Barton, *The role of radiotherapy in cancer treatment: Estimating optimal utilization from a review of evidence-based clinical guidelines, Cancer* **104** (2005) 1129.
4. S M Hashemi, B Hashemi-Malayeri, G Raisali, P Shorkani, and A A Sharifi, *A study of the photoneutrons dose equivalent resulting from a saturne 20 medical linac using Monte Carlo method, Nukleonika* **52** (2007) 39.
5. E B Podgorsak, Radiation oncology physics: a handbook for teachers and students, Vienna: International Atomic Energy Agency (2005).
6. International Atomic Energy Agency. Absorbed dose determination in photon and electron beams: an international code of practice. Technical Report Series TRS-277 (2^{nd} edition). IAEA, Vienna (1997).
7. S Jan, D Benoit, E Becheva, T Carlier, F Cassol, P Descourt, T Frisson, L Grevillot, L Guigues, L Maigne, and C Morel, GATE V6: a major enhancement of the GATE simulation platform enabling modelling of CT and radiotherapy, Phys Med Biol **56** (2011) 881.
8. J M Verburg, H A Shih, and J Seco, *Simulation of prompt gamma-ray emission during proton radiotherapy, Phys Med Biol* **57** (2012) 5459.
9. H Paganetti, *Advancing (proton) radiation therapy. Int J Radiat Oncol Biol Phys* **87** (2013)871.
10. P Andreo, *Monte Carlo simulations in radiotherapy dosimetry, Radiat Oncol* **13** (2018) 121
11. A Brahme and P Andreo, *Dosimetry and Quality Specification of High Energy Photon Beams, Acta Radiologica: Oncology* **25** (1986) 213. doi: 10.3109/02841868609136408
12. P Andreo, *On the beam quality specification of high-energy photons for radiotherapy dosimetry*, *Med Phys* **27** (2000) 434. doi: 10.1118/1.598892
13. T C F Fonseca *et al*., *MCMEG: Simulations of both PDD and TPR for 6MV LINAC photon beam using different MC codes, Radiation Physics and Chemistry* **140** (2017) 386. doi:10.1016/2017.03.048
14. J Wulff, J T Heverhagen, and K Zink, *Monte -Carlo-based perturbation and beam quality correction factors for thimble ionization chambers in high-energy photon beams, Phys Med Biol* **53** (2008) 2823. doi: 10.1088/0031-9155/53/11/005
15. A Baumgartner, A Steurer, and F J Maringer, *Simulation of photon energy spectra from Varian 2100C and 2300C/D Linacs: Simplified estimates with PENELOPE Monte Carlo models, Applied Radiation and Isotopes* **67** (2009) 2007.
16. D M González-Castaño, G H Hartmann, F Sánchez-Doblado, F Gómez, R P Kapsch, J Pena, R Capote, *The determination of beam quality correction factors: Monte Carlo simulations and measurements*, *Phys Med Biol* **54** (2009) 4723. doi: 10.1088/0031-9155/54/15/006
17. J Schuemann, S Dowdell, C Grassberger, C H Min, and S Paganetti, *Site-specific range uncertainties caused by dose calculation algorithms for proton therapy, Phys Med Biol* **59** (2014) 4007.
18. D A Granville and G O Sawakuchi, *Comparison of linear energy transfer scoring techniques in Monte Carlo simulations of proton beams*, *Phys Med Biol* **60** (2015) 283.
19. J Perl, J Shin, J Schuemann, B Faddegon, and H Paganetti, *TOPAS: an innovative proton Monte Carlo platform for research and clinical applications, Med Phys* **39** (2012) 6818.
20. J Schuemann, A L McNamara, J Ramos-Méndez, J Perl, K D Held, H Paganetti, S Incerti, and B Faddegon, *TOPAS-nBio: An Extension to the TOPAS Simulation Toolkit for Cellular and Sub-cellular Radiobiology, Radiat Res* **191** (2019) 125.
21. J K Shultis and R E Paw, *An MCNP primer. Kansas State University*, USA (2011). https://www.mne.k-state.edu/~jks/MCNPprmr.pdf
22. D B Pelowitz, *MCNPX user's manual*, version 2.6.0, 2005; Los Alamos National Laboratory
23. P Andreo, D T Burns, K Hohfeld, M S Huq, T Kanai, F Laitano, V Smyth, and C Vynckier, *absorbed dose determination in external beam radiotherapy: an international code of practice for dosimetry based on standards of absorbed dose to water. Technical Report Series TRS- 398. Vienna: International Atomic Energy Agency* (2000)
24. C M Ma and A E Nahum, *Monte Carlo calculated stem effect corrections for NE2561 and NE2571 chambers in medium-energy X-ray beams, Phys Med Biol* **40** (1995) 63. doi: 10.1088/0031-9155/40/1/006
25. ICRP committee 3 task group, P. Grande and M.C.O'Riordan, Data for protection against ionizing radiation from external sources: supplement to ICRP publication **15**, ICRP-21, International Commission on Radiological Protection, Pergamon press (1971).